TWMS J. App. and Eng. Math. V.11, N.3, 2021, pp. 893-905

RADIAL BASIS FUNCTION GENERATED FINITE DIFFERENCE METHOD FOR THE SOLUTION OF SINH-GORDON EQUATION

J. RASHIDINIA[1], M. N. RASOULIZADEH[1], §

Abstract. Accuracy of radial basis functions (RBFs) is increased as the shape parameter decreases and produces an ill-conditioned system. To overcome such difficulty, the global stable computation with Gaussian radial basis function-QR (RBF-QR) method was introduced for a limited number of nodes. The main aim of this work is to develop the stable RBF-QR-FD method in order to obtain numerical solutions for the $(1+2)$-dimensional nonlinear sinh-Gordon (ShG) equation. The efficiency and accuracy of the presented approach are tested by three examples. A comparison between our results and the three methods such as, RBFs collocation based on Kansa's (RBFK) approach, RBF-Pseudo spectral (RBFPS) and moving least squares (MLS) methods are shown. Furthermore, the stability analysis is proven.

Keywords: Radial basis function(RBF), RBF-QR method, RBF-QR-FD method, sinh-Gordon(ShG) equation, Stability analysis.

AMS Subject Classification: 65M06, 65M12, 65M70, 65M20.

1. Introduction

Many phenomena in applied sciences specially physics and engineering sciences are modelled by non-linear evolution equations, such as the sinh-Gordon equation that appears in the propagation of flaxen in Josephson junctions between two superconductors [27, 9, 29, 30]. The nonlinear partial differential equations (PDEs) appear in differential geometry, solid state physics, integrable quantum field theory, fluid dynamics, nonlinear optics and dislocation in materials [1, 31, 20].
Suppose, $\Omega \cup \partial\Omega$ be a bounded and closed set in $\mathbb{R}^2$, and Ω and $\partial\Omega$ are including the internal and the boundary points, respectively. In this study, we investigate the numerical solution of $(1+2)$-dimensional sinh-Gordon equation on the region $\Omega \cup \partial\Omega$ in the following form,

$$\begin{aligned} \frac{\partial^2 u(x,y,t)}{\partial t^2} &- \bigtriangledown^2 u(x,y,t) + \sinh(u(x,y,t)) \\ &= f(x,y,t), \quad (x,y) \in \Omega, \quad 0 < t \leq T, \end{aligned} \tag{1a}$$

[1] School of Mathematics, Iran University of Science and Technology, Tehran, 16844-13114, Iran.
e-mail: rashidinia@iust.ac.ir; ORCID: https://orcid.org/0000-0002-9177-900X.
e-mail: mnrasoulizadeh@mathdep.iust.ac.ir; ORCID: https://orcid.org/0000-0001-8420-5414.

§ Manuscript received: August 4, 2019; accepted: December 20, 2019.
TWMS Journal of Applied and Engineering Mathematics, Vol.11, No.3

with the initial conditions:

$$u(x,y,0) = g_1(x,y), \qquad (x,y) \in \Omega \cup \partial\Omega, \tag{1b}$$

$$u_t(x,y,0) = g_2(x,y), \qquad (x,y) \in \Omega \cup \partial\Omega, \tag{1c}$$

and the boundary condition

$$u(x,y,t) = \Psi(x,y,t), \quad (x,y) \in \partial\Omega,\ 0 < t \leq T. \tag{1d}$$

Where f, g_1, g_2 and Ψ are known continues functions and $\bigtriangledown^2 = \frac{\partial^2}{\partial x^2} + \frac{\partial^2}{\partial y^2}$ is the Laplace operator.

Analytical methods are incapable of obtaining the solution to most PDEs and so the numerical methods to solve them have been widely developed [17, 18, 12, 10, 19, 14].

In the recent two decades, RBFs meshfree collocation methods have been widely used for obtaining the numerical solutions of PDEs [25, 6, 5, 24, 13, 21]. Some of important advantages of using RBFs method are spectral convergence rates, geometrical flexibility, computing derivatives and the ease of implementation in high dimensions. Although RBFs methods have a spectral accuracy, they often have a large linear system with dense, ill-condition and full matrices. To overcome such difficulties, local RBF-FD methods were used [32, 2, 15, 4, 23, 22]. These methods have a sparse matrices and well conditioned system. The best accuracy of RBFs is often obtained when the flat RBFs are used, meaning that the shape parameter of RBFs becomes small. In practice, when the shape parameter decreases, the arising coefficient matrix becomes very ill-conditioned. To solve such dificulties the RBF-QR method was introduced for flat Gaussian RBFs [8, 7, 11]. The main purpose of this work is to develop the local RBF-QR-FD method to solve ShG equation as a time-dependent PDEs and doing a comparison with methods in [3]. When the number of nodes are more than thousands, the system matrix becomes ill-conditioned and not stable for time dependent PDEs. Thus, we use RBF-QR-FD method which is computing the weights by RBF-QR method instead of RBFs.

2. Collocation methods

Let $X = \{\underline{x}_1, \underline{x}_2, \cdots, \underline{x}_N\} \subseteq \mathbb{R}^d$, be a set of N distinct points with given scalar values f_i for $i = 1, 2, ..., N$.

2.1. **RBF collocation method.**

The RBF interpolation is defined as

$$s(\underline{x}, \varepsilon) = \sum_{j=1}^{N} \lambda_j \phi_j(\underline{x}), \tag{2}$$

where $\phi_j(\underline{x}) = \phi(||\underline{x} - \underline{x}_j||, \varepsilon)$, $\|.\|$ is the Euclidean norm, ε is the shape parameter and ϕ is the radial function. To determine $\{\lambda_j\}_{j=1}^{N}$, the collocation method is used.

$$s(\underline{x}_i, \varepsilon) = f_i, \qquad i = 1, \cdots, N. \tag{3}$$

The Eq. (3) leads to a linear system of equations as

$$A_\phi \, \lambda = f, \tag{4}$$

where

$$\lambda = \begin{bmatrix} \lambda_1 \\ \lambda_2 \\ \vdots \\ \lambda_N \end{bmatrix}, \quad f = \begin{bmatrix} f_1 \\ f_2 \\ \vdots \\ f_N \end{bmatrix}, \quad A_{\phi,ij} = \phi_j(\underline{x}_i), \quad i, j = 1, \cdots, N.$$

The non-singularity of the matrix A_ϕ for some RBFs were shown by Micchelli in [16].

2.2. **RBF-QR collocation method.** The best accuracy in Eq. (2) is often obtained by RBFs when the shape parameter ϵ is small. But in practice, when the shape parameter decreases toward zero, the matrix A_ϕ in Eq. (4) becomes nearly singular and ill-conditioned. To overcome such difficulty, the RBF-QR method provided well-conditioned algorithm for Gaussian RBFs, $\phi(r) = e^{-(\varepsilon r)^2}$. For this purpose, in the RBF-QR method, an expansion of the Gaussian RBFs basis in terms of combination of Chebyshev polynomials, powers of polynomial and trigonometric functions truncated at $M \geq N$ has been used as:

$$\begin{bmatrix} \phi_1(\underline{x}) \\ \phi_2(\underline{x}) \\ \vdots \\ \phi_N(\underline{x}) \end{bmatrix} \approx \underbrace{\begin{bmatrix} c_1(\underline{x}_1) & c_2(\underline{x}_1) & \dots & c_M(\underline{x}_1) \\ c_1(\underline{x}_2) & c_2(\underline{x}_2) & \dots & c_M(\underline{x}_2) \\ \vdots & \vdots & \vdots & \vdots \\ c_1(\underline{x}_N) & c_2(\underline{x}_N) & \dots & c_M(\underline{x}_N) \end{bmatrix}}_{C} \underbrace{\begin{bmatrix} d_1 & 0 & \dots & 0 \\ 0 & d_2 & \dots & 0 \\ \vdots & \vdots & \vdots & \vdots \\ 0 & 0 & \dots & d_M \end{bmatrix}}_{D} \begin{bmatrix} V_1(\underline{x}) \\ V_2(\underline{x}) \\ \vdots \\ V_M(\underline{x}) \end{bmatrix}. \tag{5}$$

In the above equation, the elements of the matrix $D_{M\times M}$, $d_k = O(\epsilon^{2m_k})$ and $(m_k \leq m_{k+1})$, and the elements of $C_{N\times M}$ and $V_{M\times 1}$ are $O(1)$ and $M \geq N$ (for more details see [7, 11]). Matrix C is factorized as $C = QR = Q(R_1, R_2)$, where R_1 is the upper triangular matrix contains N first columns of R and R_2 contains the remaining $(M - N)$ columns. The diagonal matrix D partitioned as diagonal blocks D_1 and D_2 of size $N \times N$ and $(M - N) \times (M - N)$ respectively. Now, new bases $\psi_j(\underline{x})$ instead of $\phi_j(\underline{x})$ are obtained as follows:

$$\begin{bmatrix} \psi_1(\underline{x}) \\ \psi_2(\underline{x}) \\ \vdots \\ \psi_N(\underline{x}) \end{bmatrix} = D_1^{-1} R_1^{-1} Q^T \begin{bmatrix} \phi_1(\underline{x}) \\ \phi_2(\underline{x}) \\ \vdots \\ \phi_N(\underline{x}) \end{bmatrix} \approx \begin{bmatrix} I_N & \tilde{R} \end{bmatrix} \begin{bmatrix} V_1(\underline{x}) \\ V_2(\underline{x}) \\ \vdots \\ V_M(\underline{x}) \end{bmatrix}, \tag{6}$$

where $\tilde{R} = D_1^{-1} R_1^{-1} R_2 D_2$ is the correction matrix that dues to scaling the coefficients included only non-negative powers of ε. By using transpose of Eq. (6) at all nodes $\underline{x}_i, i = 1, \cdots, N$, interpolation matrix according to new basis $\psi_j(\underline{x})$ can be computed as $A_\psi = V \begin{bmatrix} I_N \\ \tilde{R}^T \end{bmatrix}$, with the elements $a_{ij} = \psi_j(\underline{x}_i)$ and $v_{ij} = v_j(\underline{x}_i)$.

Thus, like Eqs.(2) and (4) in RBF method, interpolation formula and system matrix of the RBF-QR method are as follows:

$$s(\underline{x}, \varepsilon) = \sum_{j=1}^{N} \mu_j \psi_j(\underline{x}), \qquad A_\psi \, \mu = f, \tag{7}$$

where $\mu = \begin{bmatrix} \mu_1 \cdots \mu_N \end{bmatrix}^T$ is the unknown coefficients vector of RBF-QR interpolation method that is computed from the above system.

From Eq. (6) the action of a linear differential operator can be computed by the RBF-QR basis. Suppose $\mathcal{L}$ be a differential linear operator. Since $\tilde{R}$ is independent of $\underline{x}$, then it is possible to obtain $\mathcal{L}\psi_j(\underline{x})$ from Eq. (6) as

$$\begin{bmatrix} \mathcal{L}\,\psi_1(\underline{x}) \\ \mathcal{L}\,\psi_2(\underline{x}) \\ \vdots \\ \mathcal{L}\,\psi_N(\underline{x}) \end{bmatrix} = \begin{bmatrix} I_N & \tilde{R} \end{bmatrix} \begin{bmatrix} \mathcal{L}\,V_1(\underline{x}) \\ \mathcal{L}\,V_2(\underline{x}) \\ \vdots \\ \mathcal{L}\,V_M(\underline{x}) \end{bmatrix}. \tag{8}$$

2.3. **RBF-FD collocation method.** Suppose $I_i = \{\underline{x}_{i_1}, \underline{x}_{i_2}. \cdots \underline{x}_{i_{n_i}}\}$ be a stencil of $\underline{x}_i$ and $\mathcal{L}$ be a linear differential operator. We want to find $w = (w_1, w_2, \cdots, w_{n_i})$ such that

$$\mathcal{L}\, u(\underline{x}_i) = \sum_{j=1}^{n_i} w_j u(x_{i_j}), \tag{9}$$

where $\underline{x}_i = \underline{x}_{i_1}$ is the center node of stencil I_i. By using $\phi_{i_j}(x) = \phi(\|\underline{x} - \underline{x}_{i_j}\|)$, $j = 1, \cdots, n_i$, instead of $u(x)$ in Eq.(9), the weights can be computed from the following system:

$$A_\phi\, \underline{w} = \underline{l}\,, \tag{10}$$

where

$$\underline{w} = \begin{bmatrix} w_1 \\ w_2 \\ \vdots \\ w_{n_i} \end{bmatrix}, \underline{l} = \begin{bmatrix} \mathcal{L}\phi_{i_1}(\underline{x})|_{\underline{x}=\underline{x}_i} \\ \mathcal{L}\phi_{i_2}(\underline{x})|_{\underline{x}=\underline{x}_i} \\ \vdots \\ \mathcal{L}\phi_{i_{n_i}}(\underline{x})|_{\underline{x}=\underline{x}_i} \end{bmatrix}, \quad A_{\phi,rs} = \phi_{i_r}(\underline{x}_{i_s}), \quad r,\, s = 1, \cdots, n_i. \tag{11}$$

The weights $w_1, w_2, \cdots w_{n_i}$ can be determined from the above system.

2.4. **RBF-QR-FD collocation method.** The best accuracy of RBF-FD method in Eq. (9) is often obtained when ϵ is small, but the matrix A_ϕ in Eq. (10), becomes nearly singular and ill-conditioned. To overcome such difficulty, in the RBF-QR-FD method RBF-QR bases $\psi_{i_j}(\underline{x})$ and $\mathcal{L}\,\psi_{i_j}(\underline{x})$ from Eqs. (6) and (8) are used instead of Eq. (11). Thus

$$A_\psi\, \underline{w}_\psi = \underline{l}_\psi\,, \tag{12}$$

where

$$\underline{w}_\psi = \begin{bmatrix} w_1 \\ w_2 \\ \vdots \\ w_{n_i} \end{bmatrix}, \underline{l}_\psi = \begin{bmatrix} \mathcal{L}\psi_{i_1}(\underline{x})|_{\underline{x}=\underline{x}_i} \\ \mathcal{L}\psi_{i_2}(\underline{x})|_{\underline{x}=\underline{x}_i} \\ \vdots \\ \mathcal{L}\psi_{i_{n_i}}(\underline{x})|_{\underline{x}=\underline{x}_i} \end{bmatrix}, \quad A_{\psi,rs} = \psi_{i_r}(\underline{x}_{i_s}), \quad r,\, s = 1, \cdots, n_i. \tag{13}$$

The weights $\underline{w}_\psi$ in Eq. (13) that computed by RBF-QR bases, are the RBF-QR-FD weights.

3. Description of the Method

The implementation details of the RBF-QR-FD method for obtaining numerical solutions of ShG equation are described in this section.
Firstly, $m+1$ distinct points $t_j = jk, j = 0, 1, \cdots, m$ with time step k are chosen. Then, the central FD and θ-weighted ($0 < \theta \leq \frac{1}{2}$) methods are applied over three consecutive time steps t_{j-1}, t_j , t_{j+1} on Eq.(1a) as

$$\frac{u^{j-1} - 2\,u^j + u^{j+1}}{k^2} - \left(\theta \bigtriangledown^2 u^{j+1} + (1-2\theta) \bigtriangledown^2 u^j + \theta \bigtriangledown^2 u^{j-1}\right) + \sinh(u^j) = f(x, y, t_j), \quad for\ \underline{x} = (x, y) \in \Omega, \tag{14a}$$

$$u^j = \Psi(x, y, t_j), \quad for\ \underline{x} = (x, y) \in \partial\Omega, \tag{14b}$$

where $j = 0, 1, \cdots, (m-1)$ and$w^j = u(\underline{x}, t_j) = u(x, y, t_j)$.
Eq. (14a) can be rewritten as:

$$\Big(1 - \theta\, k^2\ \bigtriangledown^2\Big) u^{j+1} = \Big(2 + (1-2\theta)\, k^2\ \bigtriangledown^2\Big) u^j - \Big(1 - \theta\, k^2\ \bigtriangledown^2\Big) u^{j-1}$$
$$- k^2\, \sinh(u^j) + k^2\, f(x, y, t_j), \quad for\ \underline{x} = (x, y) \in \Omega. \tag{15}$$

Now, N distinct collocation nodes $X = \{\underline{x}_1, \underline{x}_2, \cdots, \underline{x}_N\}$ are chosen in set $\Omega \cup \partial\Omega$ in which $\underline{x}_i = (x_i, y_i),\ i = 1, \cdots, N_1$ are the N_1 interior points and $\underline{x}_i, i = N_1 + 1, \cdots, N$ are the N_2 boundary points.
For each point $\underline{x}_i$, stencil $I_i = \{\underline{x}_j \in X : \|x_j - x_i\| \le R\} = \{\underline{x}_{i_1}, \underline{x}_{i_2}, \cdots, \underline{x}_{i_{n_i}}\}$ in support radius R is chosen. Let's assume $\underline{x}_i = \underline{x}_{i_1}\ (i = i_1)$ without loss of generality. For each node $\underline{x}_i$ and its stencil I_i, the weights $\underline{w}_{xx,i} = [w_{xx,i1}, \cdots, w_{xx,in_i}]^T$ and $\underline{w}_{yy,i} = [w_{yy,i1}, \cdots, w_{yy,in_i}]^T$ corresponding to $\frac{\partial^2}{\partial x^2}$ and $\frac{\partial^2}{\partial y^2}$ will be determined by using RBF-QR-FD method Eq. (12). Thus the weights $\underline{w}_i = [w_{i1}, \cdots, w_{in_i}]^T$ for $\bigtriangledown^2$ can be determined by summing up $\underline{w}_{xx,i}$ and $\underline{w}_{yy,i}$ as

$$\bigtriangledown^2 u^v(\underline{x}_i) = \sum_{s=1}^{n_i} w_{is}\, u^v_{i_s}, \quad i = 1, \cdots, N_1,\ v = j-1, j, j+1, \tag{16}$$

where $u^v_{i_s} = u(\underline{x}_{i_s}, t_v)$. The weights w_{is} are only dependent on stencil nodes. Applying the collocation methods on interior nodes in Eq. (15) and using Eq. (16) concluded that

$$u_i^{j+1} - \theta\, k^2 \Big(\sum_{s=1}^{n_i} w_{is}\, u_{i_s}^{j+1}\Big) = 2u_i^j + (1-2\theta)\, k^2 \Big(\sum_{s=1}^{n_i} w_{is}\, u_{i_s}^j\Big)$$
$$- \left(u_i^{j-1} - \theta\, k^2 \Big(\sum_{s=1}^{n_i} w_{is}\, u_{i_s}^{j-1}\Big)\right) - k^2 \sinh(u_i^j) + k^2\, f(x_i, y_i, t_j). \tag{17}$$

Eq.(17) and Eq.(14b) lead to the following $N \times N$ system:

$$(1 - \theta\, k^2\, w_{i1}) u_i^{j+1} - (\theta\, k^2\, w_{i2}) u_{i_2}^{j+1} - \cdots - (\theta\, k^2\, w_{in_i}) u_{i_{n_i}}^{j+1} =$$
$$\Big(2 + (1-2\theta)\, k^2\, w_{i1}\Big) u_i^j + ((1-2\theta)\, k^2\, w_{i2}) u_{i_2}^j + \cdots + ((1-2\theta)\, k^2\, w_{in_i}) u_{i_{n_i}}^j$$
$$- \Big((1 - \theta\, k^2\, w_{i1}) u_i^{j-1} - (\theta\, k^2\, w_{i2}) u_{i_2}^{j-1} - \cdots - (\theta\, k^2\, w_{in_i}) u_{i_{n_i}}^{j-1}\Big)$$
$$- k^2\, \sinh(u_i^j) + k^2\, f(x_i, y_i, t_j), \qquad i = 1, \cdots, N_1, \tag{18a}$$

$$u_i^{j+1} = \Psi(x_i, y_i, t_{j+1}), \qquad i = N_1 + 1, \cdots, N. \tag{18b}$$

By partitioning the vector $U^{j+1} = [u_1^{j+1}, u_2^{j+1}, \cdots, u_N^{j+1}]^T = [U_1^{j+1}\ , U_2^{j+1}]^T$, where $U_1^{j+1} = [u_1^{j+1}, u_2^{j+1}, \cdots, u_{N_1}^{j+1}]^T$ and $U_2^{j+1} = [u_{N_1+1}^{j+1}, \cdots, u_N^{j+1}]^T$ correspond to the internal and boundary nodes, the matrix form of Eq.(18) will be written as:

$$U_2^{j+1} = Si^{j+1},$$
$$A_1\, U_1^{j+1} = B_1\, U_1^j - A_1\, U_1^{j-1} - S^j + F^j$$
$$+ B_2\, U_2^j - A_2\, (U_2^{j+1} + U_2^{j-1}), \quad j = 1, 2, \cdots, (m-1), \tag{19}$$

where sparse matrices $A_{N\times N}$ and $B_{N_1\times N}$ with blocks $A_{N\times N} = \begin{bmatrix} A_1 & A_2 \\ 0 & I_{N_2} \end{bmatrix}$, $B_{N_1\times N} = \begin{bmatrix} B_1 & B_2 \end{bmatrix}$ correspond to internal and boundary points, and $N_1 \times 1$ known vectors S^j, Si^{j+1}

and F^j are as follows:

$$\begin{aligned}
&A_{ii} = 1 - \theta\, k^2\, w_{i1}, \quad B_{ii} = 2 + (1-2\theta)\, k^2\, w_{i1},\\
&A_{i\,i_s} = -\theta\, k^2\, w_{is}, \quad B_{i\,i_s} = (1-2\theta)\, k^2\, w_{is},\\
&S_i^j = k^2\, \sinh(u_i^j), \quad F_i^j = k^2\, f(x_i, y_i, t_j),\\
&i = 1, \cdots, N_1\,, \quad s = 2, \cdots n_i, \quad j = 1, 2, \cdots, (m-1),
\end{aligned} \tag{20}$$

$$A_{ii} = 1, \quad Si_i^{j+1} = \Psi(x_i, y_i, t_{j+1}), \quad i = N_1 + 1, \cdots, N,\ j = 1, 2, \cdots, (m-1).$$

The other elements of vectors and matrices are equal zero.
When in Eq. (18a) $j = 0$, Eq.(1c) and central FD method at $t = 0$ are used to remove $u_{i_s}^{-1}$. Thus,

$$u_{i_s}^{-1} = u_{i_s}^1 - 2\, k\, g_2(\underline{x}_{i_s}), \quad i = 1, \cdots, N,\ s = 1, \cdots n_i. \tag{21}$$

By substituting Eq. (21) into Eq. (18a) for $j = 0$, the matrix form of linear systems at the time level $t_0 = 0$ will be obtained as:

$$\begin{aligned}
U_2^1 &= Si^1,\\
(2A_1)\, U_1^1 &= B_1\, U_1^0 + G^0 - S^0 + F^0 + B_2\, U_2^0 - (2A_2)\, U_2^1,
\end{aligned} \tag{22}$$

where $G_i^0 = 2k\,(1 - k^2\theta w_{i1})\, g_2(\underline{x}_{i_1}) - 2\theta k^3 \sum_{s=2}^{n_i} w_{is}\, g_2(\underline{x}_{i_s})$, $i = 1, \cdots, N_1$ and the other vectors and matrices are as in Eq. (20) with $j = 0$.
Therefore, for applying RBF-QR-FD method to solve ShG equation, first we use the Eq. (22) to start the method and then by using Eq. (19), the result at any time level j can be obtained.

Remark 3.1. *If $i_s \in I_i$, $\|\underline{x}_{i_s} - \underline{x}_i\| \le R$ then $i \in I_{i_s}$. Since w_{is} only depends on distance between $\underline{x}_i$ and $\underline{x}_{i_s}$, the matrix A_1 is symmetric and so its eigenvalues are real.*

4. Stability analysis

In this section the stability analysis of the presented method is investigated. The Eq. (19) can be written as

$$U_1^{j+1} = A_1^{-1}\, B_1\, U_1^j - I\, U_1^{j-1} + A_1^{-1}\, b^j, \tag{23}$$

where $b^j = -\,S^j + F^j + B_2\, U_2^j - A_2\left(U_2^{j+1} + U_2^{j-1}\right)$. Also Eq. (23) can be written as,

$$\begin{bmatrix} U_1^{j+1} \\ U_1^j \end{bmatrix} = \begin{bmatrix} A_1^{-1}\, B_1 & -I_{N_1} \\ I_{N_1} & 0 \end{bmatrix} \begin{bmatrix} U_1^j \\ U_1^{j-1} \end{bmatrix} + \begin{bmatrix} A_1^{-1} & 0 \\ 0 & 0 \end{bmatrix} \begin{bmatrix} b^j \\ 0 \end{bmatrix}. \tag{24}$$

By setting $V^{j+1} = \begin{bmatrix} U_1^{j+1} \\ U_1^j \end{bmatrix}$, $P = \begin{bmatrix} A_1^{-1}\, B_1 & -I_{N_1} \\ I_{N_1} & 0 \end{bmatrix}$ and $\overline{b}^j = \begin{bmatrix} A_1^{-1} & 0 \\ 0 & 0 \end{bmatrix} \begin{bmatrix} b^j \\ 0 \end{bmatrix}$, Eq. (24) can be written as the two time levels form as:

$$V^{j+1} = P\, V^j + \overline{b}^j, \quad j = 0, 1, \cdots, m-1. \tag{25}$$

Theorem 4.1. *Suppose that spectral radius of matrix P is defined by $\rho(P) = \max\{|\lambda| : P\, x = \lambda x,\ x \neq 0\,\}$. If $\theta = \frac{1}{2}$ and $\rho(A_1^{-1}) \le 1$, then presented method Eq. (25) is stable.*

Proof. Choosing $\theta = \frac{1}{2}$ in Eq. (20) concludes that $B = 2\, I$, thus $P = \begin{bmatrix} 2\, A_1^{-1} & -I \\ I & 0 \end{bmatrix}$. Suppose μ is an arbitrary eigenvalue of A_1 (since A_1 is symmetric thus μ is real) and so

$\frac{1}{\mu}$ is an arbitrary eigenvalue of A_1^{-1}. Therefore, the corresponding eigenvalue of P is the eigenvalue of the matrix $H = \begin{bmatrix} \frac{2}{\mu} & -1 \\ 1 & 0 \end{bmatrix}$[28]. So,

$$det(P - \lambda I) = det(H - \lambda I) = \lambda^2 - \frac{2}{\mu}\lambda + 1 = 0,$$

thus $\lambda_1, \lambda_2 = \frac{1}{\mu} \pm \frac{\sqrt{1-\mu^2}}{\mu}$ are the eigenvalues of P. On the other hand, since $\lim_{k\to 0} A = I$ and determinant is continuous function of k, then $\lim_{k\to 0} \mu = 1$, thus for small values of k, $\mu > 0$. If $0 < \mu < 1$, then $\rho(P) = \max\{|\lambda_1|, |\lambda_2|\} \geq \frac{1}{\mu} > 1$, and our method is not stable. But if $\rho(A_1^{-1}) \leq 1$, then $\frac{1}{\mu} \leq 1$ and $\mu \geq 1$. Hence, the eigenvalues of P are complex, i. e., $\lambda_1, \lambda_2 = \frac{1}{\mu} \pm i\,\frac{\sqrt{\mu^2-1}}{\mu}$ and $\rho(P) = max\{|\lambda_1|, |\lambda_2|\} = 1$ and the proof is complete. □

Theorem 4.2. *Our presented method for small values of k is stable.*

Proof. Since, $\lim_{k\to 0} A_{1,ii} = \lim_{k\to 0}(1-\theta\, k^2\, w_{i1}) = 1$, $\lim_{k\to 0} A_{1,ii_j} = \lim_{k\to 0}(-\theta\, k^2\, w_{ij}) = 0$, $\lim_{k\to 0} B_{1,ii} = \lim_{k\to 0}(2 + (1-\theta)\, k^2\, w_{i1}) = 2$, and $\lim_{k\to 0} B_{1,ii_j} = \lim_{k\to 0}((1-\theta)\, k^2\, w_{ij}) = 0$. Then, $\lim_{k\to 0} A_1 = I$, $\lim_{k\to 0} B_1 = 2\,I$ and $P = \begin{bmatrix} 2\,I & -I \\ I & 0 \end{bmatrix}$. So, as we shown in the previous theorem, $H = \begin{bmatrix} 2 & -1 \\ 1 & 0 \end{bmatrix}$ and then $det(P - \lambda\, I) = det(H - \lambda\, I) = \lambda^2 - 2\,\lambda + 1 = 0$. Therefore, the eigenvalues of P are $\lambda_1, \lambda_2 = 1$ and $\rho(P) = 1$, then the proof is complete. □

5. Numerical illustrations

To confirm the accuracy and efficiency of the proposed method, three examples are considered in this section. The comparison of L_∞ and RMS errors and condition number between three methods in [3], RBFK, RBFPS and MLS methods; and presented method is given. The convergence behaviors and computational orders are computed by the following norm functions:

(1) $L_\infty = \|\underline{U}_e - \underline{U}\|_\infty = max_{1\leq i\leq N_1} |\underline{U}_e(\underline{x}_i) - \underline{U}(\underline{x}_i)|$,

(2) $RMS = \left(\frac{1}{N_1} \sum_{i=1}^{N_1} (\underline{U}_e(\underline{x}_i) - \underline{U}(\underline{x}_i))^2 \right)^{\frac{1}{2}}$,

(3) $C - order = \log\left(\frac{E_j}{E_{j+1}}\right) / \log\left(\frac{k_j}{k_{j+1}}\right)$,

where $\underline{x}_i$, $i = 1, \cdots, N$ are the collocation nodes, $\underline{U}_e$ and $\underline{U}$ are the exact and computational values of $u(x, y, t)$ respectively and E_j is the L_∞ error respect to k_j or h_j.
The Matlab software and the kdtree package by Guy Shechter [26] for constructing stencils are used to apply RBF-QR-FD method. Moreover, we use $\theta = \frac{1}{12}$, the famous Numerov's method and Gaussian RBFs in all examples. It should be mentioned that, the proper initial and boundary conditions have been obtained from the exact solutions.

Example 5.1. *Two soliton solutions of ShG equation:*

$$u(x, y, t) = \sin(t)(sech^2(5 - x - y) + sech^2(5 + x + y)), \quad (x, y) \in \Omega, \quad t \geq 0.$$

The comparison of L_∞ error between presented method and three methods in [3] *with $k = 1/100$ on $\Omega = [0, 1] \times [0, 1]$ at $T = 1$ has been shown in the Table 1. In the Table*

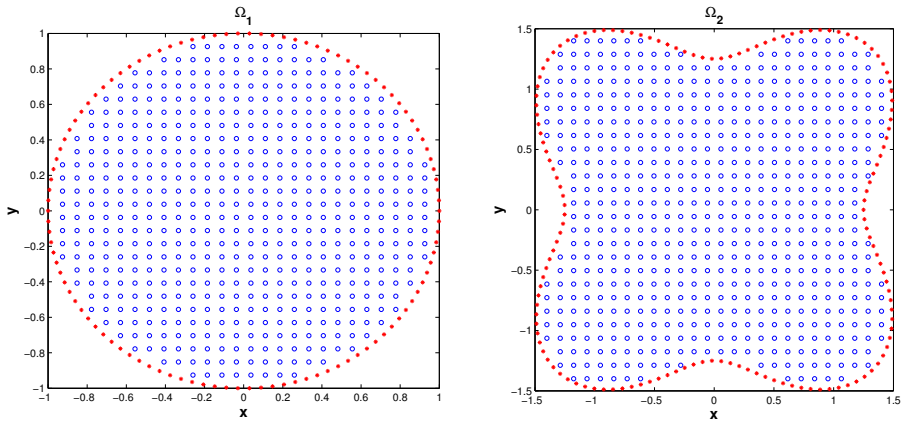

FIGURE 1. Considered domains.

2, the effect of the number of stencil nodes (n_s), for example 5.1 has been reported. It is clear from the Table 2 that by increasing n_s, the accuracy increases. The graphs of approximation solutions and point-wise errors of presented method on domains Ω_1 and Ω_2 (Fig. 1) at $T = 1$ and 10 have been shown in Fig. 2. They have confirmed the ability of accuracy and geometrical flexibility of RBF-QR-FD method.

TABLE 1. Errors and computational order with $k = 1/100$, $\epsilon = 0.4$ and $n_s = 49$ on $[0, 1] \times [0, 1]$ at $T = 1$ for Example 5.1.

h	MLS		RBFK		RBFPS		RBF-QR-FD	
	L_∞	C-order	L_∞	C-order	L_∞	C-order	L_∞	C-order
1/5	$2.7839E-03$	–	$2.5885E-03$	–	$2.5885E-03$	–	$2.5574e-06$	–
1/10	$2.0984E-04$	3.7297	$6.6647E-04$	1.9575	$6.6647E-04$	1.9575	$1.9088e-06$	0.4220
1/15	$5.3085E-05$	3.3898	$2.3284E-04$	2.5937	$2.3284E-04$	2.5937	$6.8233e-07$	2.5371
1/20	$4.1188E-05$	0.8820	$8.7058E-05$	3.4197	$8.7056E-05$	3.4197	$4.7970e-07$	1.2248
1/25	$3.5431E-05$	0.6747	$4.3493E-05$	3.1099	$4.3093E-05$	3.1513	$1.8391e-07$	4.2964

TABLE 2. Condition number and L_∞ and RMS errors of Example 5.1 at $T = 1$ on $[-5, 5] \times [-5, 5]$ with $h = 1/10$, $k = 1/100$, and $\epsilon = 0.8$ for different values of n_s.

n_s	$Cond(A)$	L_∞	RMS
5	1.0075	7.6751×10^{-1}	2.5836×10^{-1}
9	1.0110	1.4354×10^{-3}	5.1756×10^{-4}
13	1.0111	1.4119×10^{-3}	4.8003×10^{-4}
21	1.0134	6.4790×10^{-5}	2.1029×10^{-5}
25	1.0117	6.5054×10^{-5}	2.2411×10^{-5}
29	1.0140	6.6405×10^{-5}	1.6405×10^{-5}
37	1.0191	2.7414×10^{-5}	6.3192×10^{-6}

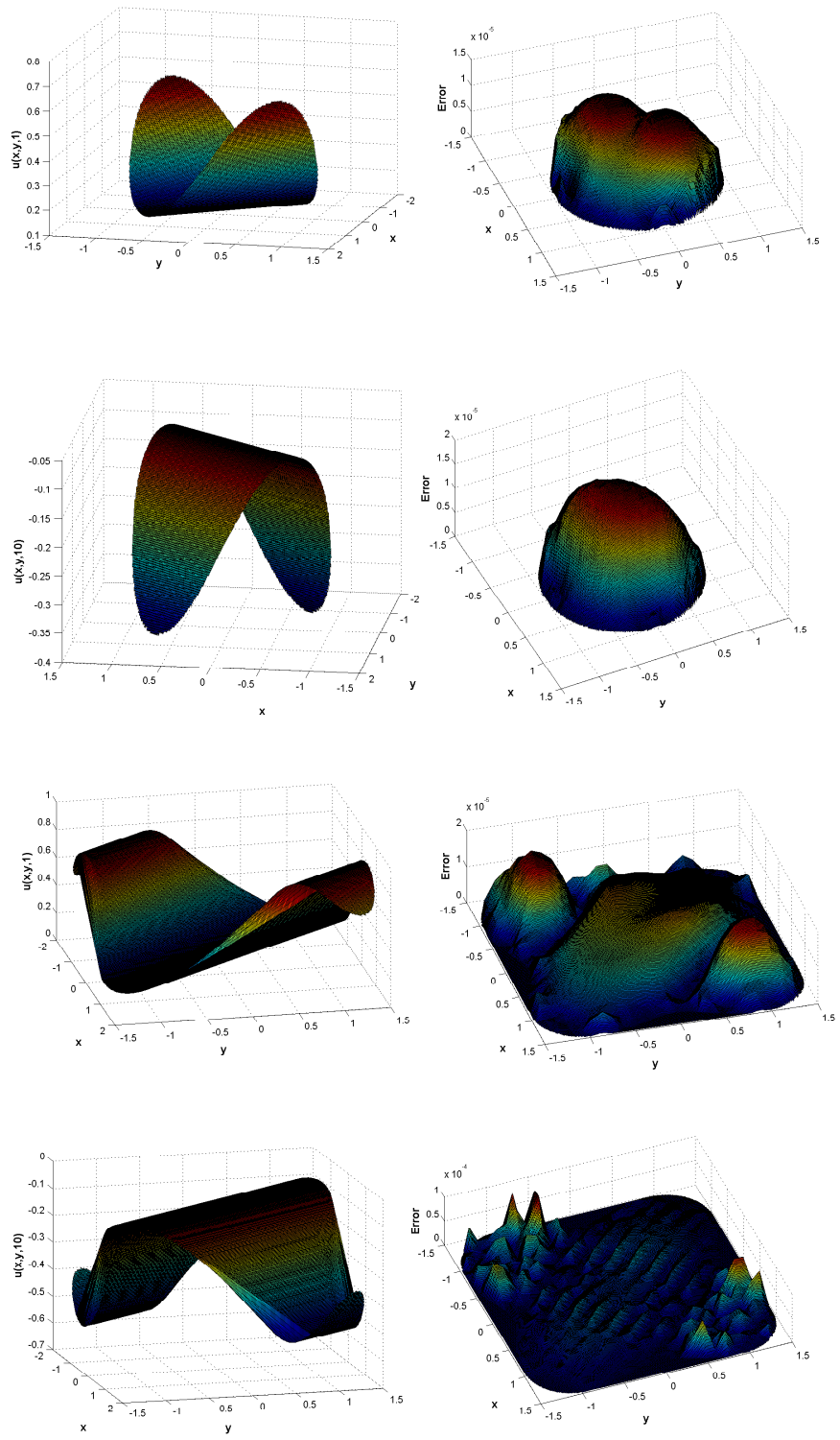

FIGURE 2. Graphs of approximatin solutions (left) and errors (right) using the RBF-QR-FD method with $\epsilon = 0.4$, $r = 2$, and $k = 1/100$ on Ω_1 (up) and Ω_2 (down) for example 5.1 at $T = 1$, 10.

TABLE 3. L_∞ error and computational order of Example 5.2 with $h = 1/5$, $\epsilon = 0.4$ on $[0,1] \times [0,1]$ at $T = 1$.

k	MLS		RBFK		RBFPS		RBF-QR-FD	
	L_∞	C-order	L_∞	C-order	L_∞	C-order	L_∞	C-order
1/10	$1.7749E-02$	–	$1.8527E-05$	–	$1.8527E-02$	–	$3.7588E-03$	–
1/20	$1.2346E-02$	0.5237	$1.2221E-02$	0.6003	$1.2221E-02$	0.6003	$7.7368E-04$	2.2805
1/40	$1.0716E-02$	0.2043	$1.1512E-02$	0.8622	$1.1512E-02$	0.8622	$2.2157E-04$	1.8040
1/80	$6.7502E-03$	0.6668	$7.6602E-03$	0.5877	$7.6602E-03$	0.5877	$4.5700E-05$	2.2775
1/160	$3.6208E-03$	0.8986	$4.2924E-03$	0.8356	$4.2924E-03$	0.8356	$1.5232E-05$	1.5851
1/320	$1.7386E-03$	1.0584	$2.1401E-03$	1.0041	$2.1401E-03$	1.0041	$1.1999E-05$	0.3442
1/640	$7.5607E-04$	1.0544	$2.9170E-04$	1.6748	$2.9170E-04$	1.6748	$1.1504E-05$	0.0608

TABLE 4. L_∞ error and condition number of Example 5.2 with $k = 1/100$, $\epsilon = 0.4$ and $n_s = 29$ on $[0,1] \times [0,1]$ at $T = 1$.

h	MLS		RBFK		RBFPS		RBF-QR-FD	
	L_∞	Cond (A)	L_∞	Cond(A)	L_∞	Cond(A)	L_∞	Cond(A)
1/5	$5.6015E-03$	$7.71E+04$	$3.4571E-03$	$3.45E+2$	$3.4571E-03$	1.25	$2.3804E-05$	1.0045
1/10	$8.4393E-03$	$6.02E+07$	$6.4590E-04$	$1.75E+3$	$6.4590E-04$	1.57	$3.6668E-05$	1.0614
1/15	$9.1597E-03$	$1.66E+10$	$2.9539E-04$	$2.95E+4$	$2.9539E-04$	2.10	$5.2778E-05$	1.0408
1/20	$9.3619E-03$	$3.02E+11$	$1.5029E-05$	$1.50E+4$	$1.5029E-05$	3.50	$3.4312E-05$	1.0760
1/25	$9.3872E-03$	$2.08E+12$	$8.9040E-05$	$8.90E+5$	$8.9040E-05$	4.97	$4.0460E-05$	1.1155

TABLE 5. L_∞ error and computational order of Example 5.3 with $r = 10$, $n_s = 25$, $\epsilon = 0.2$ and $h = 1/5$ on $[0,1] \times [0,1]$ at $T = 1$.

k	MLS		RBFK		RBFPS		RBF-QR-FD	
	L_∞	C-order	L_∞	C-order	L_∞	C-order	L_∞	C-order
1/10	$1.3740E-05$	–	$1.6663E-05$	–	$1.6663E-05$	–	$1.5272e-05$	–
1/20	$6.9876E-06$	0.9751	$1.3368E-05$	0.3179	$1.3368E-05$	0.3179	$1.2727e-06$	3.5849
1/40	$3.6663E-06$	0.9305	$1.1598E-05$	0.2049	$1.1598E-05$	0.2049	$2.2409e-07$	2.5057
1/80	$2.6158E-06$	0.4871	$1.0568E-05$	0.1342	$1.0568E-05$	0.1342	$5.6507e-08$	1.9876
1/160	$2.0845E-06$	0.3276	$1.0201E-05$	0.0509	$1.0201E-05$	0.0509	$5.6491e-08$	0.0004
1/320	$1.8165E-06$	0.1985	$1.0626E-05$	-0.05889	$1.0626E-05$	-0.05889	$5.6020e-08$	0.0121

TABLE 6. L_∞ error and condition number of Example 5.3 with $r = 1$, $n_s = 13$, $\epsilon = 0.2$ and $k = \frac{1}{320}$ on $[0,1] \times [0,1]$ at $T = 1$.

h	MLS		RBFK		RBFPS		RBF-QR-FD	
	L_∞	Cond (A)	L_∞	Cond(A)	L_∞	Cond(A)	L_∞	Cond(A)
1/5	$1.8165E-06$	$7.96E+04$	$1.0625E-05$	$5.23E+3$	$1.0626E-05$	1.00	$8.6020e-08$	1.00
1/10	$3.7664E-07$	$7.09E+07$	$6.6476E-05$	$1.54E+6$	$4.6476E-06$	1.02	$3.1998e-08$	1.00
1/15	$3.8692E-07$	$2.55E+9$	$1.6958E-06$	$2.73E+8$	$1.6958E-06$	1.04	$3.2020e-08$	1.00
1/20	$4.0596E-07$	$2.88E+10$	$6.2424E-07$	$3.88E+10$	$6.2434E-07$	1.07	$4.9050e-08$	1.00
1/25	$4.1466E-07$	$1.78E+11$	$4.0442E-07$	$4.86E+12$	$4.0359E-07$	1.12	$4.5245e-08$	1.01

Example 5.2. *Elliptical ring soliton solution of ShG equation:*

$$u(x,y,t) = 4\,\tan^{-1}(exp(t + \frac{1}{6}\sqrt{36 + 30x^2 + 12xy + 30y^2}\,)), \quad (x,y) \in \Omega, \quad t \geq 0.$$

In the Table 3, the comparison of L_∞ errors and computational order between the presented method and methods in [3] *for some values of k and $h = 1/5$ on $[0,1]$ has been presented for*

example 5.2. The condition numbers and errors has been reported in the Table 4. Tables 3 and 4 shown that the presented method is more well-conditioned than the methods in [3].

Example 5.3. *Collision of four circular solitons of ShG equation:*

$$u(x,y,t) = \tan^{-1}(exp(t + 2.29\sqrt{r + (x+3)^2 + (y+3)^2}\ )) + \tan^{-1}(exp(t+ 2.29\sqrt{r + (x+3)^2 + (y-3)^2}\ )) + \tan^{-1}(exp(t + 2.29\sqrt{r + (x-3)^2 + (y+3)^2}\ )) + \tan^{-1}(exp(t + 2.29\sqrt{r + (x-3)^2 + (y-3)^2}\ )), \quad (x,y) \in \Omega, \quad t \geq 0.$$

The comparison of L_∞ errors, computational order and condition number of system matrix between presented method and methods in [3]*, have been shown in the Tables 5 and 6. These Tables shown that it is more well conditioned than the methods in* [3].

6. Conclusion

In this work, the stable computation for numerical solution of the ShG equations using collocation method based on RBF-QR-FD has been presented. The stability analysis of this method has been proved. The efficiency of this technique was tested by three examples. The numerical results given in the previous section demonstrate a good accuracy of this method and a significant improvement in camparision with the methods in [3]. In the linear system of the RBF-QR-FD method, the sparse and n_s diagonal matrices with well conditions has been observed. So, the number of nodes can be increased to some extent.

References

[1] Albeverio, S., Høegh-Krohn, R., (1981), Stochastic methods in quantum field theory and hydrodynamics, Phys. Rep., 77(3), pp. 193–214.

[2] Bayona, V., Moscoso, M., Carretero, M., Kindelan, M., (2010), RBF-FD formulas and convergence properties, J. Comput. Phys., 229(22), pp. 8281–8295.

[3] Dehghan, M., Abbaszadeh, M., Mohebbi, A., (2015), The numerical solution of the two–dimensional sinh-gordon equation via three meshless methods, Eng. Anal. Bound. Elem., 51, pp. 220–235.

[4] Dehghan, M., Mohammadi, V., (2017), A numerical scheme based on radial basis function finite difference (RBF-FD) technique for solving the high-dimensional nonlinear schrödinger equations using an explicit time discretization: Runge–kutta method, Comput. Phys. Commun., 217, pp. 23–34.

[5] Dereli, Y., Irk, D., Dağ, İ., (2009), Soliton solutions for nls equation using radial basis functions, Chaos. Soliton. Fract., 42(2), pp. 1227–1233.

[6] Fasshauer, G. E., (2007), Meshfree Approximation Methods with Matlab, 6, World Scientific publications.

[7] Fornberg, B., Larsson, E., Flyer, N., (2011), Stable computations with gaussian radial basis functions, SIAM J. Sci. Comput., 33(2), pp. 869–892.

[8] Fornberg, B., Piret, C., (2007), A stable algorithm for flat radial basis functions on a sphere, SIAM J. Sci. Comput., 30(1), pp. 60–80.

[9] Fu, Z., Liu, S., Liu, S., (2004), Exact solutions to double and triple sinh-gordon equations, Z. Naturforsch. C., A 59(12), pp. 933–937.

[10] Fu, Z. J., Xi, Q., Ling, L., Cao, C. Y., (2017), Numerical investigation on the effect of tumor on the thermal behavior inside the skin tissue, Int. J. Heat. Mass. Tran., 108, pp. 1154–1163.

[11] Larsson, E., Lehto, E., Heryudono, A., Fornberg, B., (2013), Stable computation of differentiation matrices and scattered node stencils based on gaussian radial basis functions, SIAM J. Sci. Comput., 35(4), pp. A2096–A2119.

[12] Lin, J., Chen, CS., Liu, CS. and Lu, J., (2016), Fast simulation of multi-dimensional wave problems by the sparse scheme of the method of fundamental solutions, Comput. Math. Appl., 72(3), pp. 555–567.

[13] Lin, J., Reutskiy, S. Y., Lu, J., (2018), A novel meshless method for fully nonlinear advection–diffusion-reaction problems to model transfer in anisotropic media, Appl. Math. Comput., 339, pp. 459–476.

[14] Lin, J., Zhang, C., Sun, L. and Lu, J., (2018), Simulation of seismic wave scattering by embedded cavities in an elastic half-plane using the novel singular boundary method, Adv. Appl. Math. Mech., 10(2), pp. 322–342.
[15] Martin, B., Fornberg, B., (2017), Using radial basis function-generated finite differences (RBF-FD) to solve heat transfer equilibrium problems in domains with interfaces, Eng. Anal. Bound. Elem., 79, pp. 38–48.
[16] Micchelli, Charles, A., (1984), Interpolation of scattered data: distance matrices and conditionally positive definite functions, Approximation theory and spline functions, Springer, pp. 143–145.
[17] Mohanty, RK. and Singh, S., (2011), A new high-order approximation for the solution of two-space-dimensional quasilinear hyperbolic equations, Adv. Math. Phys., 2011 , Article ID 420608, 22 pages.
[18] Mohanty, RK. and Kumar, R., (2014), A new fast algorithm based on half-step discretization for one space dimensional quasilinear hyperbolic equations, Appl. Math. Comput., 244, pp. 624–641.
[19] Mohanty, RK. and Khurana, G., (2017), A new fast numerical method based on off-step discretization for two-dimensional quasilinear hyperbolic partial differential equations, Int. J. Comp. Meth-Sing., 14(3), pp. 1750031, 1–27.
[20] Mohanty, RK. and Khurana, G., (2019), A new high accuracy cubic spline method based on half-step discretization for the system of 1D non-linear wave equations, Eng. Computation., 36(3), pp. 930–957.
[21] Nikan, O., Golbabai, A., Nikazad, T, (2019), Solitary wave solution of the nonlinear KdV-Benjamin-Bona-Mahony-Burgers model via two meshless methods. Eur. Phys. J., 134(7), pp. 367–382.
[22] Nikan, O., Machado, J. T., Golbabai, A. and Nikazad, T., (2019), Numerical investigation of the nonlinear modified anomalous diffusion process. Nonlinear Dyn., 97(4) pp. 2757–2775.
[23] Rashidinia, J., Rasoulizadeh, M. N., (2019), Numerical methods based on radial basis function-generated finite difference (RBF-FD) for solution of GKdVB equation, Wave Motion., 90, pp. 152–167.
[24] Safdari-Vaighani, A., Mahzarnia, A., (2015), The evaluation of compound options based on rbf approximation methods, Eng. Anal. Bound. Elem., 58, pp. 112–118.
[25] Sarra, S. A., (2005), Adaptive radial basis function methods for time dependent partial differential equations, Appl. Numer. Math., 54(1), pp. 79–94.
[26] Shechter, G., (2004), Matlab package kdtree.
[27] Sirendaoreji, S. J., Jiong, S., (2002), A direct method for solving sinh-gordon type equation, Phys. Lett. A., 298(2-3), pp. 133–139.
[28] Smith, G. D., (1985), Numerical solution of partial differential equations, finite difference methods, Oxford university press.
[29] Wazwaz, A. M., (2006), Exact solutions for the generalized sine-gordon and the generalized sinh-gordon equations, Chaos. Soliton. Fract., 28(1), pp. 127–135.
[30] Wazwaz, A. M., (2007), A variable separated ode method for solving the triple sine-gordon and the triple sinh-gordon equations, Chaos. Soliton. Fract., 33(2), pp. 703–710.
[31] Wazwaz, A. M., (2012), One and two soliton solutions for the sinh–gordon equation in (1+ 1),(2+ 1) and (3+ 1) dimensions, Appl. Math. Lett., 25(12), pp. 2354–2358.
[32] Wright, G. B., Fornberg, B., (2006), Scattered node compact finite difference-type formulas generated from radial basis functions, J. Comput. Phys., 212(1), pp. 99–123.

Jalil Rashidinia has been a professor in applied mathematics at the School of Mathematics, Iran University of Science and Technology (IUST), Narmak, Tehran, Iran, since 1999. He has published more than 100 research papers in various international journals. His research interests are applied mathematics, numerical analysis, numerical solution of ODE, PDE, integral equations and spline approximations. He has supervised about 100 master theses and 10 doctoral theses. .

Mohmmad Navaz Rasoulizadeh is a PhD student at the School of Mathematics, Iran University of Science and Technology (IUST), Narmak, Tehran, Iran, and also he has been a faculty member in the Department of Mathematics, Velayat University, Iranshahr, Iran, since 2006. His research interests are numerical analysis, numerical solution of PDEs and ODEs, and numerical linear algebra.